

Investigation of Base Isolated Structures Utilizing Stable Unbonded Fiber Reinforced Elastomeric Isolators

N.C. Van Engelen, D. Konstantinidis & M.J. Tait

Department of Civil Engineering, McMaster University, Hamilton, Canada



SUMMARY:

A scaled base isolated low-rise structure, utilizing *Stable Unbonded Fiber Reinforced Elastomeric Isolators* (SU-FREIs) is investigated. A SU-FREI is designed to maintain positive tangential stiffness for all levels of imposed horizontal displacement. The load-displacement behaviour of the SU-FREIs is simulated using a bilinear model calibrated with experimental test data for two different designs. One of the isolators considered has holes in the loaded surface, which serve as a means to modify the horizontal and vertical properties of the isolator. Two historical earthquake time histories are used to investigate the performance of these base isolated structures in comparison to a fixed base structure. Peak absolute acceleration, inter-storey displacement, and base shear are used as key performance indicators. Results from this study conclude that the addition of holes in the loaded surface of SU-FREIs can be used as an additional design parameter to modify the behaviour of the isolation system.

Keywords: Stable Unbonded Fiber Reinforced Elastomeric Isolator (SU-FREI), Holes, Bilinear model

1. INTRODUCTION

Fiber Reinforced Elastomeric Isolators (FREIs) are an attractive alternative to conventional Steel Reinforced Elastomeric Isolators (SREIs). The fiber reinforcement has similar tensile mechanical properties to steel, but is substantially lighter. The use of fiber reinforcement may allow for less labour intensive manufacturing and also the possibility of manufacturing large pads that can be cut to the required size (Kelly 1999). This process allows for large strip isolators to be manufactured more efficiently than strip SREIs. The application of large strip isolators allow for uniform support to be provided along walls, which reduces the requirements of a structural system to distribute the loads to isolators orientated in a grid system.

The reinforcement is orientated in alternating horizontal layers and allows a higher vertical stiffness to be obtained without compromising the low horizontal stiffness (Kelly and Konstantinidis 2011). Unlike steel reinforcement, which is rigid in both flexure and extension, the fiber reinforcement is assumed to be extensible and to provide no appreciable flexural resistance. When placed unbonded to the upper and lower supports, this results in a unique curved deformation under lateral displacement. As the lateral displacement increases, the initially vertical ends of the isolator will roll-off of the supports and form a curved profile, as shown in Fig. 1.1. This roll-off deformation will continue until the initially vertical face of the isolator comes into full contact with the upper and lower supports, fully rolling over. If the isolator retains a positive tangential stiffness throughout the displacement it is considered to be stable and is denoted as a *Stable Unbonded Fiber Reinforced Elastomeric Isolator* (SU-FREI). When full rollover of a SU-FREI occurs, the isolator begins to stiffen, which acts to restrict the maximum horizontal displacement of the isolator: a desirable feature beyond design-basis events (Toopchi-Nezhad et al. 2008b). SU-FREIs have been investigated in detail to date by Toopchi-Nezhad et al. (2008a, 2008b, 2009a, 2009b).

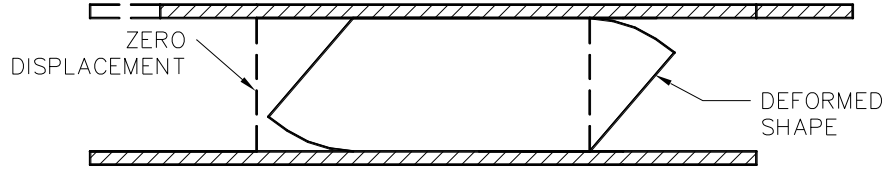


Figure 1.1. Horizontal profile of the deformed and un-deformed shape of a SU-FREI under lateral displacement

The use of larger strip isolators in lieu of smaller grid orientated isolators could potentially have an undesirably large horizontal stiffness due to the increased loaded area. An increase in horizontal stiffness decreases the shift of the fundamental period of the structure introduced by the base isolation system, which reduces the overall efficiency of the system.

A preliminary study conducted by Van Engelen et al. (2012a, 2012b) investigated the introduction of holes to the loaded surface of SU-FREIs as a means of altering the vertical and horizontal properties of the isolators. It was found that a substantial drop in the vertical stiffness and compression modulus could be obtained with relatively small amounts of area removed. The observed trends were in line with existing theory for annular FREIs (Pinarbasi and Okay 2011) and annular SREIs (Constantinou et al. 1992). The influence of the holes on the horizontal properties altered both the effective horizontal stiffness and viscous damping characteristics of the isolators. It was found that the introduction of holes increased the viscous damping ratio of the isolator while decreasing the effective horizontal stiffness. However, at displacements exceeding full rollover, a substantial increase in stiffness was observed that approached the value obtained for an unaltered strip isolator. Simultaneously, the viscous damping ratio also significantly decreased at higher displacements.

This paper presents the results of a numerical study conducted to verify the effectiveness of the modified strip isolators from Van Engelen et al. (2012a, 2012b) as a base isolation system for a low rise structure. Two SU-FREIs are considered under time histories from two historical earthquakes at scaled peak ground accelerations (PGA).

2. BILINEAR MODEL

The bilinear model, as described by Naeim and Kelly (1999), idealizes the hysteretic response of an isolator based on three parameters. These parameters are the elastic stiffness, K_1 , the post-yield stiffness, K_2 , and the characteristic strength, Q , as shown in Fig. 2.1. The effective horizontal stiffness, K_{eff} , the effective equivalent viscous damping ratio, ξ_{eff} , and Q , can be determined from experimental testing. Q is taken as the average of the absolute values of the zero displacement force intercepts, Q_1 and Q_2 in Fig.2.1. K_{eff} , taken as the secant between the peak displacements, can be expressed as:

$$K_{eff} = K_2 + \frac{Q}{v_b} \quad (2.1)$$

where v_b is the peak displacement of the hysteresis loop under consideration. Similarly, the effective viscous damping ratio is defined by:

$$\xi_{eff} = \frac{4Q(v_b - v_{b,y})}{2\pi K_{eff} v_b^2} \quad (2.2)$$

where $v_{b,y}$ is the yield displacement and the numerator represents the area contained within the hysteresis loop. The above expression can be cast in non-dimensional quantities using a non-dimensional displacement, $y = v_b/v_{b,y}$, and a non-dimensional characteristic strength, $\alpha = Q/(K_2 v_{b,y})$. The effective viscous damping ratio becomes:

$$\xi_{eff} = \frac{2\alpha(y-1)}{\pi(y+\alpha)y} \quad y \geq 1 \quad (2.3)$$

If α is constant, the above expression can be differentiated with respect to y . Setting the derivative to zero, y can be solved to yield a maximum effective viscous damping ratio located at:

$$y = 1 + (1 + \alpha)^{1/2} \quad (2.4)$$

with the value of:

$$\xi_{\max} = \frac{2\alpha}{\pi} \frac{1}{2(1+\alpha)^{1/2} + (2+\alpha)} \quad (2.5)$$

In the time history analysis, for displacements less than those corresponding to the maximum damping ratio, the damping ratio is set equal to the maximum damping ratio. Otherwise the damping is calculated from Eqn. 2.3 (Toopchi-Nezhad et al. 2009b).

The non-dimensional characteristic strength can alternatively be expressed as:

$$\alpha = \frac{K_1 - K_2}{K_2} \quad (2.6)$$

From the above equations, it is concluded that the elastic stiffness has no influence over the effective horizontal stiffness, but that it does influence the effective damping ratio. The results of this model are based on rate independent stiffness and amplitude dependent damping. The bilinear model has been previously used to model SU-FREIs by Toopchi-Nezhad et al. (2009b), and Foster (2011).

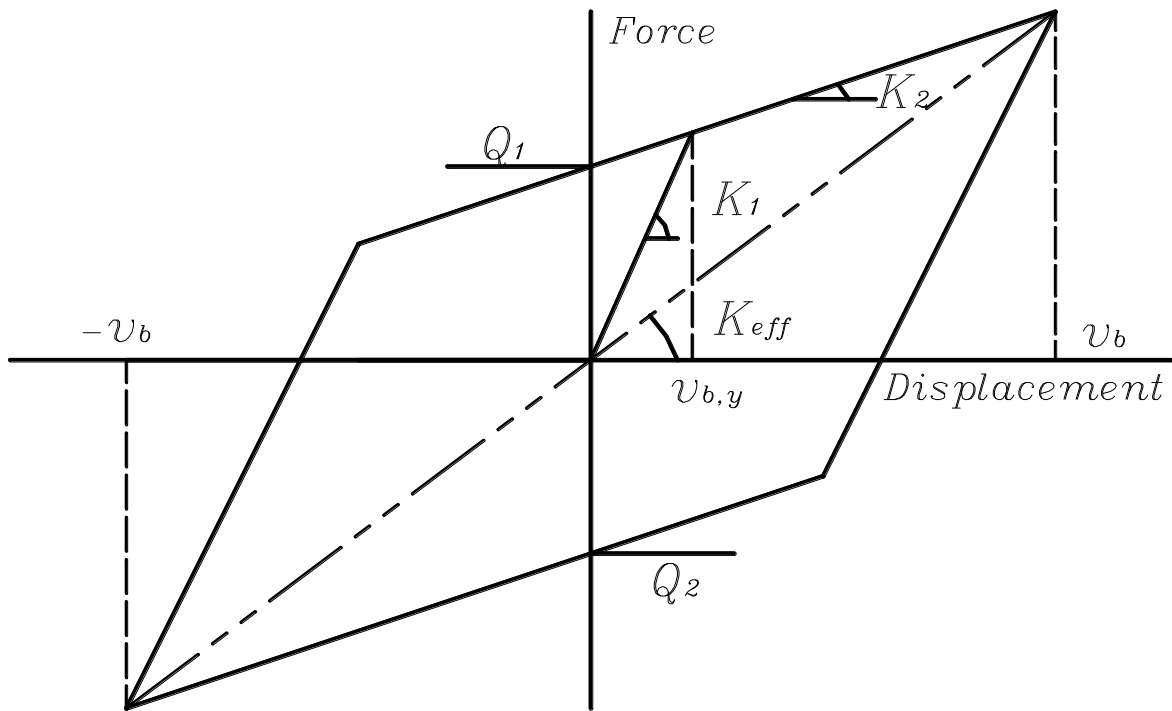


Figure 2.1. Bilinear model representation of a force-displacement hysteresis loop

3. MODEL

3.1 SU-FREI Specimens and Parameters

Two quarter scale SU-FREIs were considered in this study. The vertical and horizontal properties of these isolators were investigated in Van Engelen et al. (2012a, 2012b). The isolators contained seven elastomeric layers with a total thickness, t_r , of 19 mm. The total height of the isolator was 22 mm. The

geometry of the isolators is shown in Fig. 3.1 along with the actual specimens. Isolator B1 was the reference case with no modifications made to the loaded surface. Isolator B2 was the isolator with the largest loaded area removed of all the isolators considered in the previous studies, and was selected to represent the modified isolators for this study. Isolator B2 had two holes placed on the loaded surface, each of equal size located centrally on their respective half of the isolator. The holes resulted in a loaded area reduction of 13% for isolator B2.

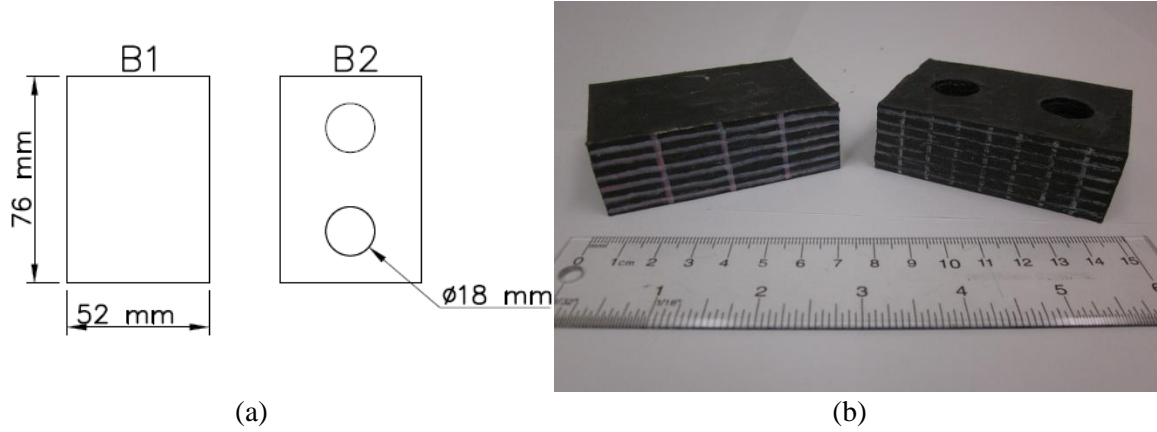


Figure 3.1. (a) Plan view of the two SU-FREIs investigated, and (b) the test specimens

Table 3.1 shows the experimentally obtained K_{eff} and ζ_{eff} for B1 and B2 along with the derived bilinear model parameters. Each isolator was tested at seven displacement amplitudes with three cycles at each amplitude as explained in the companion paper by Van Engelen et al. (2012a). For the purposes of this model, all of the values presented correspond to the first (unscragged) cycle. The decrease in K_{eff} at intermediate displacement amplitudes followed by an increase at higher displacement amplitudes is a characteristic response feature of SU-FREIs. For the isolators considered, a minimum K_{eff} occurs at 150% t_r and a maximum K_{eff} occurs at the lowest displacement amplitude, 25% t_r .

Fig. 3.2 shows the experimental hysteresis loops and bilinear model of the 100% t_r and 150% t_r cycles of isolator B1. It can be seen that the bilinear model matches the experimental hysteresis loops well at low and intermediate displacement amplitudes. However, due to the influence of the rollover, the model does not match the experimental hysteresis loops at higher displacement amplitudes, beginning at 200% t_r . Despite the discrepancy at higher displacement amplitudes, the model is still calibrated to both K_{eff} and ζ_{eff} of each hysteresis loop considered.

Table 3.1. Isolator Experimental Properties and Bilinear Model Parameters

Displacement Amplitude v_b	B1					B2				
	K_{eff} (N/mm)	ζ_{eff} (%)	K_1 (N/mm)	K_2 (N/mm)	Q (N)	K_{eff} (N/mm)	ζ_{eff} (%)	K_1 (N/mm)	K_2 (N/mm)	Q (N)
25% t_r	91.7	10.5	137.6	70.7	98.7	73.2	15.6	130.5	48.0	119.0
50% t_r	74.6	10.5	116.4	59.8	138.8	55.9	17.1	110.0	36.6	183.6
75% t_r	62.9	9.6	99.9	54.4	120.5	47.6	15.9	92.4	33.3	204.0
100% t_r	55.0	9.2	83.3	46.5	161.0	42.4	15.0	80.5	30.8	220.5
150% t_r	46.2	9.6	72.7	39.6	187.9	38.9	14.0	73.5	30.1	251.6
200% t_r	49.6	8.1	73.8	44.3	205.3	45.2	10.9	76.4	38.3	265.0
250% t_r	52.1	7.8	77.5	47.3	227.1	48.9	9.7	80.0	43.3	270.3

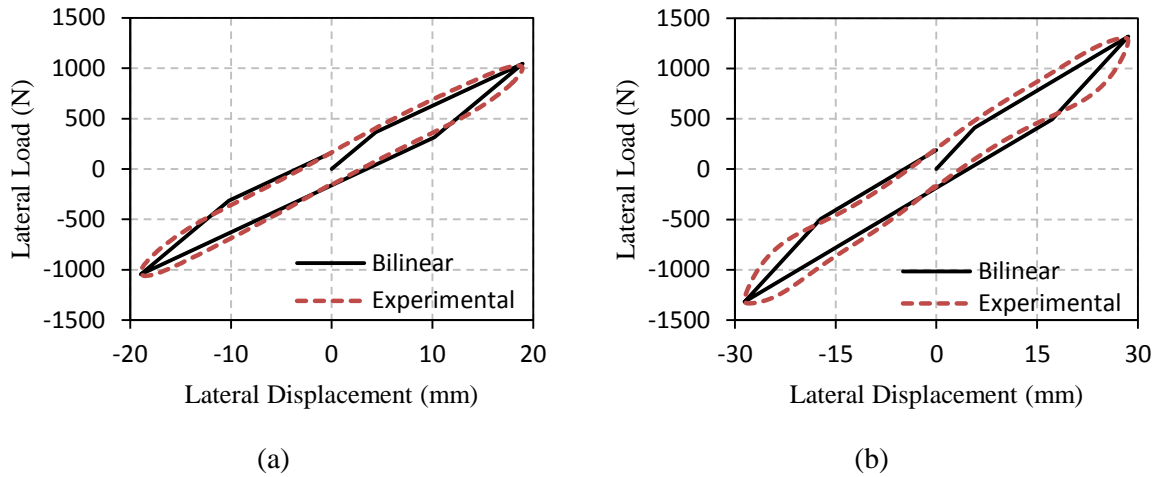


Figure 3.2. Bilinear model and experimental hysteresis loops for isolator B1 at (a) 100% t_r , and (b) 150% t_r

3.2 Structure Model

The quarter scale model base isolated structure was a modified version of the structure used by Toopchi-Nezhad et al. (2009b) and identical to the one used by Foster (2011) to conduct scaled experimental studies and subsequent model analysis. The structure was a two storey single bay moment resisting steel frame with a total weight of 32.1 kN distributed evenly over three levels, including the base isolated level.

The structure was supported by four columns, with a SU-FREI placed under each. The structure's isolator properties were assumed to be cumulative based on the experimentally determined properties. The fixed base structure had a fundamental period of 0.104 s. and an assumed damping ratio of 5%. The damping matrix was formulated using Rayleigh damping. The rotational degrees of freedom, shown in Fig. 3.3, were eliminated by employing static condensation. As described above, the mass was evenly distributed, therefore, $m_1 = m_2 = m_b = 1092$ kg.

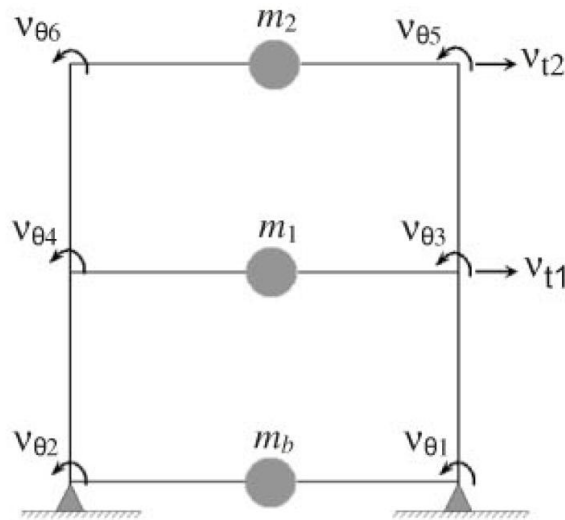


Figure 3.3. Idealized translational and rotational degrees of freedom in the structure with lumped mass (Toopchi-Nezhad et al. 2009b)

3.3 Methodology

Acceleration time histories from two historical earthquakes; the El Centro motion, recorded during the 1940 Imperial Valley earthquake; and the San Jose Santa Teresa Hills motion, recorded during the

1989 Loma Prieta earthquake, were selected for this preliminary investigation. The time histories were half-scaled in duration in order to maintain dynamic similitude. The time histories were also scaled to a PGA of 0.33 g, which corresponds to design ground motions for Montreal, Canada (NBCC 2010). The time histories used in this study are shown in Fig. 3.4.

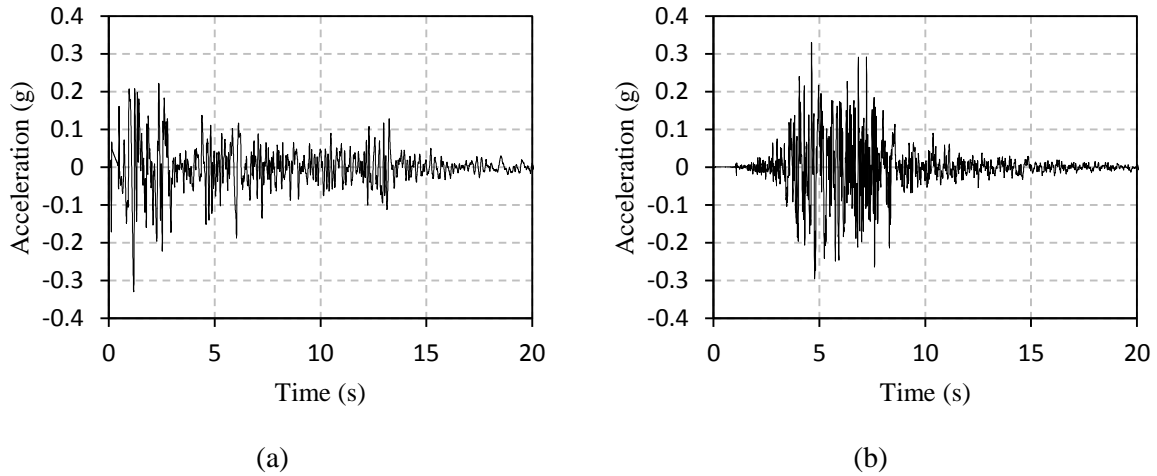


Figure 3.4. Earthquake time histories for (a) El Centro (1940), and (b) San Jose (1989) scaled to 0.33 g PGA

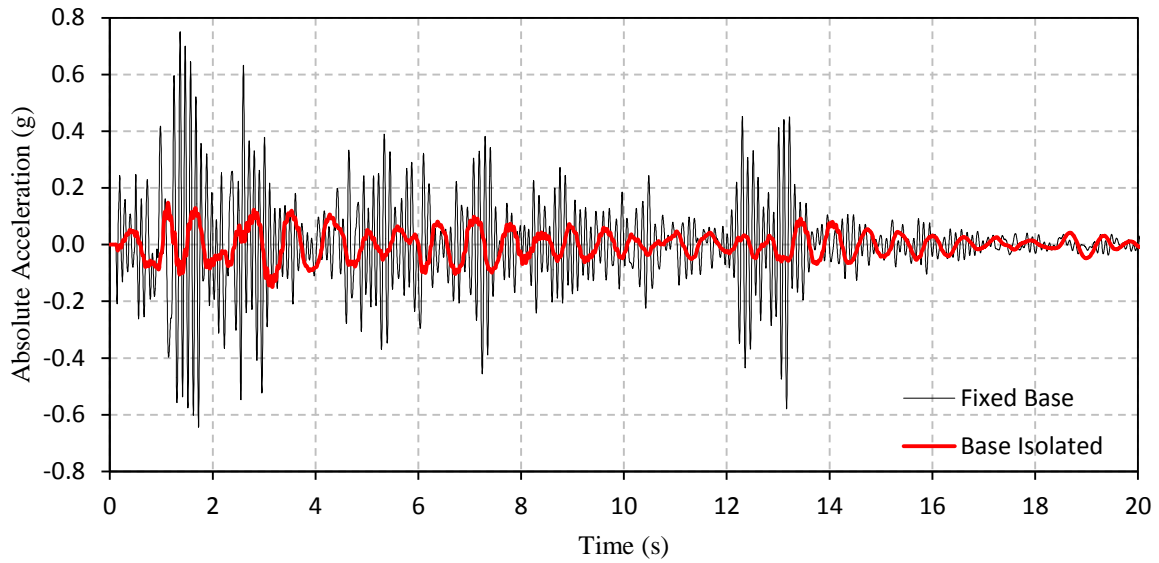
As the peak response is typically of most interest, an iterative process was employed that matches the bilinear model parameters, K_1 , K_2 , and Q , to the peak displacement from the time history analysis, $v_{b,max}$ (Toopchi-Nezhad et al. 2009b). The bilinear model parameters for each displacement amplitude of the unscragged cycle are provided in Table 3.1. The iterative procedure is as follows:

- 1) Conduct the time history analysis using the experimental values for K_1 , K_2 , and Q , corresponding to the maximum experimental displacement amplitude of 250% t_r .
- 2) Based on the calculated value of $v_{b,max}$ from the time history analysis, establish new values for K_1 , K_2 , and Q , utilizing linear interpolation between the displacement amplitudes from the experimental results.
- 3) Repeat the time history analysis to determine an updated $v_{b,max}$ and updated bilinear model parameters.
- 4) Continue the iteration until the desired convergence criteria has been met for $v_{b,max}$.

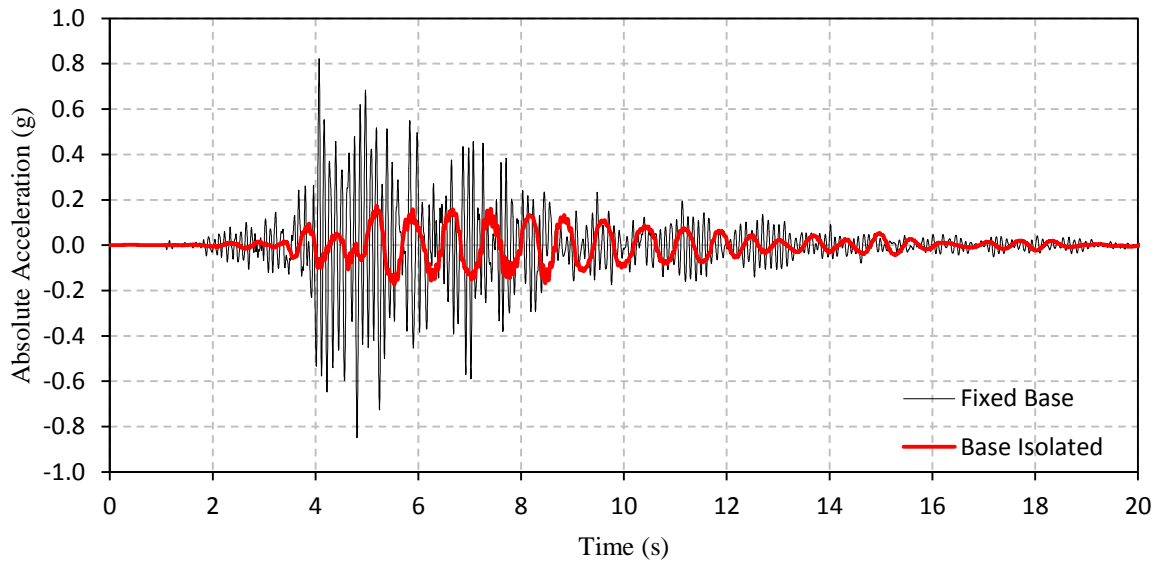
In this study, a convergence criterion of $\pm 1\%$ t_r accuracy was selected and typically achieved within five iterations. The numerical analysis of the fixed base structure does not require an iterative approach since the structure is assumed to act elastically. The isolators are assumed to be vertically stiff, and all vertical interactions are not considered.

4. NUMERICAL ANALYSIS RESULTS

The effectiveness of the base isolated system was evaluated based on three key performance indicators. The peak absolute acceleration, inter-storey displacement and drift, and base shear were investigated for each earthquake considered and compared against the values obtained from the fixed base structure analysis. The peak isolator displacement and period are also discussed. The acceleration response of the top storey for the fixed base and base isolated structures utilizing isolator B1 are shown in Fig. 3.5. The influence of the isolation system on the response can immediately be identified. The overall response is significantly lower in magnitude, and has a longer period. This differentiates the base isolated structure from the high frequency response of the fixed base structure.



(a)



(b)

Figure 3.5. Top storey acceleration response to (a) El Centro and (b) San Jose, base isolated with B1 isolators

4.1 Peak Absolute Acceleration

The peak absolute accelerations are summarized in Table 4.1. In all cases, the peak absolute acceleration response is a maximum at the top storey. A maximum fixed base response of 0.75 g and 0.85 g were observed for El Centro and San Jose, respectively. By comparison, the peak absolute acceleration response of the base isolated structure, with either isolator, is substantially lower. A peak absolute acceleration response of 0.15 g and 0.17 g was observed from isolator B1 for El Centro and San Jose, respectively. The base isolated response ranged between 16% and 32% of the fixed base response.

It can be observed that the peak response between storeys is relatively consistent for the base isolated structure, whereas a substantial increase exists between storeys for the fixed base structure. The first mode of a base isolated structure is dominated by deformation at the isolation level, while the upper storeys of the supported structure remain relatively rigid. Therefore the structure has similar peak absolute accelerations at different storeys, and substantially lower response than a fixed base structure.

Only a small increase in peak acceleration was observed at the second storey for the base isolated structure.

Isolator B2 outperformed isolator B1 in all cases considered, as indicated by the lower peak absolute accelerations. The more favourable results of isolator B2 are contributed to its lower effective horizontal stiffness in comparison to B1. A lower effective horizontal stiffness increases the fundamental period of the base isolated structure, resulting in a further shift out of the high energy range of an earthquake, thus further reducing the demand on the structure.

Table 4.1. Peak Absolute Accelerations

Record	Storey	Fixed Base (FB)		B1		B2	
		(g)	(g)	(% of FB)	(g)	(% of FB)	
El Centro	1	0.43	0.14	32	0.11	27	
	2	0.75	0.15	20	0.13	17	
San Jose	1	0.56	0.16	29	0.13	24	
	2	0.85	0.17	20	0.14	16	

4.2 Peak Inter-Storey Displacement and Drifts

The maximum inter-storey displacement occurred over the first storey of the structure, as indicated in Table 4.2. This is attributed to a larger cumulated shear at this level, and the fact that the design of the first storey and second storey of the test structure were identical. The maximum inter-storey displacement for the fixed base structure was 1.11 mm and 1.31 mm for El Centro and San Jose, respectively. Based on a storey height of 776 mm, the maximum drift was 0.14% and 0.17%, respectively. The low observed drifts were attributed to the high stiffness of the structure.

Regardless of the low inter-storey displacements and drifts, the base isolated structure displayed a desirable reduction with values ranging between 17% and 28% of the fixed base values. Similar to the peak absolute acceleration response, it can be observed that the peak inter-storey displacements for isolator B2 were lower than isolator B1 in all instances.

Table 4.2. Peak Inter-Storey Displacements and Drifts

Record	Storey	Fixed Base (FB)		B1			B2		
		(mm)	(%)	(mm)	(%)	(% of FB)	(mm)	(%)	(% of FB)
El Centro	0 - 1	1.11	0.14	0.31	0.04	28	0.25	0.03	22
	1 - 2	0.90	0.12	0.19	0.02	21	0.16	0.02	18
San Jose	0 - 1	1.31	0.17	0.36	0.05	27	0.29	0.04	22
	1 - 2	1.02	0.13	0.22	0.03	21	0.18	0.02	17

4.3 Peak Isolator Displacement

The peak isolator displacement is shown in Table 4.3. Isolator B1 and B2 had a peak displacement of 24.92 mm (131% t_r) and 23.30 mm (122% t_r), respectively. Comparing the peak isolator displacement to the inter-storey displacements, it is evident that the displacement response of the base isolated structure was dominated by the base isolated layer. The responses of these isolators were in the optimum displacement amplitude range for the records considered. The effective horizontal stiffness is a minimum at 150% t_r and begins to increase substantially at higher amplitudes. The peak isolator displacement defines the design requirements for a seismic gap around the structure.

Table 4.3. Peak Isolator Displacement, v_b

Record	B1		B2	
	(mm)	(% t_r)	(mm)	(% t_r)
El Centro	19.36	102	17.48	92
San Jose	24.92	131	23.30	122

4.4 Peak Base Shear

The peak base shear values are shown in Table 4.4. The peak base shear for the fixed base structure was 12.7 kN and 15.0 kN for El Centro and San Jose, respectively. The base isolated structure ranged between 19% and 24% of the fixed base values. These peak base shear values correspond to an isolator displacement of 24.58 mm (129% t_r) and 21.04 mm (110% t_r) for isolator B1 and B2, respectively, for the San Jose record. Similar to the other key performance indicators, isolator B2 resulted in a larger reduction in base shear than isolator B1.

The base shear coefficient, c , is the base shear normalized by the total weight of the structure. The base shear coefficient was 0.39 for El Centro, and 0.47 for San Jose for the fixed base structure. The base isolated base shear was substantially lower, ranging between 0.08 and 0.11, with isolator B2 having the lowest overall values.

Table 4.4. Peak Base Shear

Record	Fixed Base (FB)		B1			B2		
	(kN)	c	(kN)	c	(% of FB)	(kN)	c	(% of FB)
El Centro	12.7	0.39	3.1	0.10	24	2.5	0.08	20
San Jose	15.0	0.47	3.6	0.11	24	2.9	0.09	19

4.5 Fundamental Period

The desirable performance of the base isolated structure observed above can be attributed to the increase in the fundamental period, and superior damping characteristics. In the bilinear model, the fundamental period of the base isolated structure is a function of isolator displacement due to changes in the effective stiffness. Table 4.5 shows the range of the fundamental period obtained for each isolator and the fixed base structure. It can be seen that the base isolated fundamental period was approximately six to nine times larger than the fixed base structure. The bilinear model will yield the minimum fundamental period up to the yield displacement, and then increase to the maximum fundamental period at the peak isolator displacement for each record.

Table 4.5. Fundamental Period (s)

Record	Fixed Base	B1		B2	
		Min	Max	Min	Max
El Centro	0.104	0.624	0.769	0.619	0.858
San Jose	0.104	0.647	0.808	0.646	0.893

5. CONCLUSIONS

This paper investigated the performance of base isolated structures under earthquake ground excitation using SU-FREIs with holes in the loaded surface. The peak acceleration, inter-storey displacement, and base shear were investigated in comparison to a fixed base structure as key performance indicators of the base isolation system.

Two different SU-FREI designs were considered. The isolator's horizontal and vertical properties were previously investigated experimentally (Van Engelen et al. 2012a, 2012b). Isolator B2 was unique due to the removal of area from the loaded surface through the introduction of two holes, each of equal size. The introduction of holes to the loaded surface is intended to serve as a method to better optimize the horizontal and vertical properties of large strip isolators. The isolators were numerically analysed with an iterative approach to the bilinear model, which has rate independent stiffness, and amplitude dependent damping. The model was calibrated based on the experimentally determined isolator properties.

It was found that the base isolated structure significantly outperformed the fixed base structure in all of the key performance indicators. The response of the base isolated structures ranged between

approximately 20% and 30% of the fixed base structure's response. Isolator B2, which contained holes, had a lower response than B1 in all of the key performance indicators. This was attributed primarily to the lower effective horizontal stiffness of isolator B2. The lower stiffness acts to increase the isolator period and thus further reduce the response of the structure. With proper design consideration, the introduction of holes to the loaded surface of SU-FREIs can be used as an additional design parameter to better optimize the system behaviour.

Further investigation is required to evaluate the performance of other reduced loaded area SU-FREIs, and also to evaluate the performance of the isolators in the perpendicular direction. Preliminary findings indicate that introducing holes to the loaded surface can equip the designer with substantial control over the horizontal and vertical properties. Numerical analysis of these isolators has indicated that the isolation potential of SU-FREIs with holes in the loaded surface is not compromised. This type of base isolation system provides notable benefits over a traditional fixed base structure. These collective results indicate that strip isolators are a promising approach to seismic isolation.

ACKNOWLEDGEMENT

This research was carried out as part of the mandate of the McMaster University Centre for Effective Design of Structures and funded through the Natural Sciences and Engineering Research Council of Canada (NSERC) and the Ontario Ministry of Economic Development and Innovation.

REFERENCES

- Constantinou, M.C., Kartoum, A. and Kelly, J.M. (1992). Analysis of Compression of Hollow Circular Elastomeric Bearings. *Engineering Structures*. **14:2**, 103-111.
- Foster, B.A.D. (2011). Base Isolation Using Stable Unbonded Fibre Reinforced Elastomeric Isolators (SU-FREI). M.A.Sc. thesis, McMaster University.
- Kelly, J.M. (1999). Analysis of Fiber-reinforced Elastomeric Isolators. *Journal of Seismology and Earthquake Engineering*. **2:1**, 19-34.
- Kelly, J.M. and Konstantinidis, D. (2011). *Mechanics of Rubber Bearings for Seismic Isolation and Vibration Isolation*, John Wiley & Sons, Chichester, U.K.
- Naeim, F. and Kelly, J.M. (1999). *Design of Seismic Isolated Structures: From Theory to Practice*, John Wiley & Sons, United States of America.
- NBCC. (2010), National Building Code of Canada, National Research Council of Canada, Ottawa, Canada.
- Pinarbasi, S. and Okay, F. (2011). Compression of Hollow-circular Fiber-reinforced Rubber Bearings. *Structural Engineering and Mechanics*. **38:3**, 361-384.
- Toopchi-Nezhad, H., Tait, M.J. and Drysdale, R.G. (2008a). Testing and Modeling of Square Carbon Fiber-reinforced Elastomeric Seismic Isolators. *Structural Control and Health Monitoring*. **15**, 876-900.
- Toopchi-Nezhad, H., Tait, M.J. and Drysdale, R.G. (2008b). Lateral Response Evaluation of Fiber-Reinforced Neoprene Seismic Isolators Utilized in an Unbonded Application. *Journal of Structural Engineering*. **134:10**, 1627-1637.
- Toopchi-Nezhad, H., Drysdale, R.G. and Tait, M.J. (2009a). Parametric Study on the Response of Stable Unbonded-Fiber Reinforced Elastomeric Isolators (SU-FREIs). *Journal of Composite Materials*. **43:15**, 1569-1587.
- Toopchi-Nezhad, H., Drysdale, R.G. and Tait, M.J. (2009b). Simplified Analysis of a Low-Rise Building Seismically Isolated with Stable Unbonded Fiber Reinforced Elastomeric Isolators. *Canadian Journal of Civil Engineering*. **34**, 1182-1194.
- Van Engelen, N.C., Tait M. J. and Konstantinidis, D. (2012a). Horizontal Behaviour of Stable Unbonded Fiber Reinforced Elastomeric Isolators (SU-FREIs) with Holes. *15th World Conference on Earthquake Engineering*. Lisbon, Portugal, September 24-28, 2012.
- Van Engelen, N.C., Tait M. J. and Konstantinidis, D. (2012b). Vertical Response Behaviour of Stable Unbonded Fiber Reinforced Elastomeric Isolators (SU-FREIs) with Holes in the Loaded Surface. *Canadian Society for Civil Engineering Annual General Conference*. Edmonton, Alberta, Canada. June 6-9, 2012.